JMEPEG (1996) 5:353-364

Reheat Cracking Studies on Simulated Heat-Affected Zones of CrMoV Turbine Rotor Steels

J.E. Indacochea and G.S. Kim

The reheat cracking susceptibility of the heat-affected zone (HAZ) of a CrMoV turbine rotor steel was investigated. Two base materials, one with a coarse-grain (155 μm) and the other with a fine-grain (55 μm) microstructure, were submitted to Gleeble HAZ weld simulations. Three peak temperatures were utilized: 1350, 1150, and 950 °C. Some samples were single cycled, and others were exposed to a double cycle. The samples that were double cycled experienced a second peak temperature 150 to 250 °C lower than the first peak temperature. The samples were then stressed in bending for different amounts and stress relieved under load to determine their reheat cracking susceptibility. All samples were metallurgically evaluated before and after the reheat cracking test. It was found that the prior-austenite grain size of the original base metal did not influence the reheat cracking susceptibility, but increases in peak temperature did. It was observed that the grain size and grain matrix microhardness that developed after the Gleeble cycles affected reheat cracking. It was found that reheat cracking did not occur when the microhardness was below 350 DPH and the prior-austenite grain size was less than about 80 μm.

Keywords
carbide precipitation, CrMoV steels, Gleeble, HP/IP turbine rotor, reheat cracking

1. Introduction

STEAM TURBINE rotors are among the most critical and highly stressed components in the electric power industries. Although relatively few instances of catastrophic rotor bursts have occurred, such failures have resulted in long forced outages and severe economic disadvantages to the affected utilities. To forestall the possibility of a catastrophic burst, utilities typically retire several rotors annually, according to equipment manufacturer recommendations. However, the criteria and methodology for determining which rotors should be retired are proprietary and vary among manufacturers. The turbine rotors used in the electric power industry are fabricated from heat-treatable CrMoV steels for high-pressure stages and NiCrMoV steels for intermediate- and low-pressure stages. Because they operate at elevated temperatures over periods of many years, these rotors may become metallurgically damaged in ways that lead to cracking.

One of the most important questions confronting utilities in the near future undoubtedly will concern replacement of these high- and intermediate-pressure turbine rotors due to several life-limiting failures. Most rotor deteriorations result from low-cyclic fatigue (Ref 1-3). Although rotors are designed for fatigue resistance, this potential problem is inherent in all rotating equipment, and even careful design has not prevented its occurrence. A second reason for failures is creep-induced cracking. Although most turbine materials are intended to operate below the range of temperatures known to cause significant creep, there are some locations where creep that can lead to cracking regularly occurs. A third reason for failure is known to be the susceptibility of rotors to temper embrittlement due to impurity elements such as phosphorus, sulfur, arsenic, tin, and antimony.

When a turbine rotor becomes significantly damaged, a utility is forced to remove the unit from service and purchase power at a substitutional cost until a replacement rotor is ready. Weld repair of turbine rotors, if feasible, offers an opportunity for significant savings to electric utilities and their customers. Such repairs could reduce replacement costs by restoring a cracked rotor and returning it to service until a new rotor arrives. Usually weld repair of a damaged region is carried out by a "build-up" technique or, if necessary, by replacing the local interstage section with a new forging welded to the old rotor (Ref 4). This technological advance, which has favorable cost benefits, also possesses inherent risks. Repair by welding versus rotor replacement has a benefit/cost ratio that often exceeds 6 to 1 (Ref 5). The weld repair alternative also offers substantial savings in reduced downtime that can extend the benefit/cost ratio beyond 20 to 1 (Ref 5). The favorable financial benefits are somewhat offset by an element of risk associated with weld repair.

Although the potential advantages of weld repair are recognized, such procedures traditionally have not been considered. One reason is that the compositions of rotor alloys are not considered amenable to welding (Ref 6). These steels are often quenched and tempered to achieve the levels of strength required for service. As a consequence, carbon contents up to 0.35% are typical, as are moderate levels of alloys such as nickel, chromium, molybdenum, and vanadium added for hardenability. These alloy additions have been known to lead to cracking during the welding process or shortly thereafter.

A number of reports (Ref 7, 8) have been published regarding cases of serious failures in the heat-affected zone (HAZ) or weld metal of joints of cast and forged assemblies for electric power equipment made of CrMoV steels. It is recognized that when steel is welded in heavy sections, it is often necessary to perform a stress-relief heat treatment to relieve the welding residual stresses. This procedure restores notch toughness in both the weld metal and the HAZ, which prevents cracking of the

J.E. Indacochea, University of Illinois at Chicago, Chicago, Illinois, USA; and **G.S. Kim,** Soon Chun Hyang University, Onyang, Chungnam, Korea.

weld joint during subsequent exposure to service. This type of failure associated with residual stresses, called "reheat cracking," is characterized by the development of intergranular cracks in the coarse-grain regions of the HAZ, or occasionally in the weld metal, and can occur when a welded assembly is reheated to relieve the residual stresses or during service at elevated temperatures.

CrMoV steels are known to be susceptible to reheat cracking at the coarse-grain regions of the HAZ. This intergranular cracking along prior-austenite grain boundaries is apparently caused, in part, by precipitation of vanadium carbides within the grains of this region, which increases the strength of the grains relative to the grain-boundary cohesion strength (Ref 9). This cracking also accompanies the plastic relaxation of residual stress by creep and is a manifestation of poor creep ductility. Under the action of stress, strain takes place by grain-boundary sliding, leading to cavitations and grain-boundary failure at low ductilities.

The objective of this study was to examine the susceptibility of 1.0Cr-1.0Mo-0.25V turbine rotor steels to reheat cracking when welded. The assessment of resistance to reheat cracking was carried out with simulated HAZs that were produced with a thermomechanical weld simulator (Gleeble 1500, Dynamic Systems Inc., Poestenkill, NY). This investigation was undertaken to better understand the mechanism of reheat cracking in conjunction with the welding process, so as to possibly optimize the heat treatment and welding parameters to reduce or eliminate reheat cracking. It was discovered in earlier studies that reheat cracking did not occur after welding and stress relief of the multipass weld coupons fabricated from this rotor steel (Ref 10). It was concluded then that grain refinement of the coarse-grain heat-affected zone (CGHAZ), compared to the base metal, reduced susceptibility to reheat cracking due to improved toughness. Evaluation of a commercial narrow-gap weldment of the same rotor steel also revealed no reheat cracking. It was found that a butter weld pass had been deposited to further refine the CGHAZ (Ref 11).

This investigation was conducted using two different grain sizes of the same rotor material. The purpose was to establish a connection between original base-metal grain size, CGHAZ grain size, and cracking susceptibility.

2. Experimental Work

Test specimens were machined from a retired high/intermediate-pressure (HP/IP) rotor steel that had been in service for 20 years. Its composition is shown in Table 1. Two grain structures were utilized. The grain size of the as-retired rotor (155 μm) was defined as coarse. Material from the same rotor steel was submitted to intercritical heat treatments to obtain the fine-grain (55 μm) microstructure.

The experimental work followed in this study is summarized in Fig. 1. The Gleeble thermal cycles to which these test specimens were submitted are shown in Table 2. For the samples submitted to a double cycle, the second peak temperatures were 800, 950, and 1050 °C, corresponding to the peak temperatures of 950, 1100, and 1350 °C.

Evaluation of the reheat crack susceptibility was conducted with a three-point-bend notch-opening stress-relaxation test fixture (Fig. 2a), where the samples were loaded in the fixture to a selected notch-opening displacement (NOD), measured with a dial gage. The loaded sample with the fixture was placed

Table 1 Chemical composition of rotor steel

Element	Weight percent
Carbon	0.36
Manganese	0.86
Phosphorus	0.016
Sulfur	0.013
Silicon	0.22
Nickel	0.10
Chromium	1.08
Molybdenum	1.10
Vanadium	0.25

Table 2 Gleeble thermal cycles of test specimens prior to bend test

Base metal	Coarse grain (155 μm) Fine grain (55 μm)
Peak temperature, °C	950, 1150, and 1350
Cycle	Single and double
Preheat temperature, °C	250
Heating rate, °C/s	200
$\Delta T_{800\text{-}500}$, s	50
Cooling rate, °C/s	50
Interpass temperature, °C	250
Postweld heat temperature, °C	677

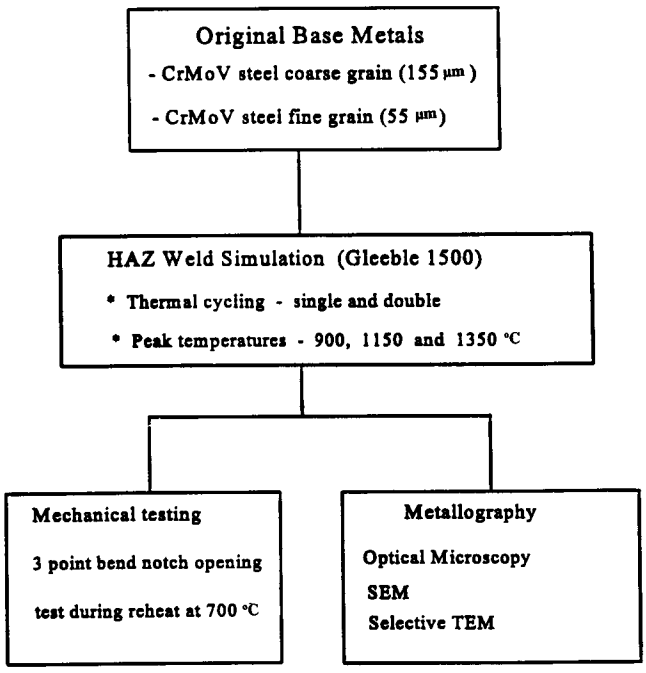

Fig. 1 Experimental work for simulated HAZs in assessing reheat cracking

in the furnace and heat treated in an argon atmosphere using a thermal cycle described in Fig. 2(b). Following the reheat crack test, all samples were removed and observed for evidence of cracking visually and using an optical microscope. The test samples evaluated were then impact fractured at liquid nitrogen temperatures after the reheat crack test and examined with a scanning electron microscope (SEM). Selective transmission electron microscopy (TEM) was performed to analyze the role of the carbides. For all microscopic observations, standard metallographic procedures were followed in the preparation of specimens. Microhardness measurements were also performed.

3. Results and Discussion

From earlier investigations (Ref 10, 11) it was determined that multipass welding refined the grain in the CGHAZ compared to the original grain size of the rotor steel. This refinement was found to be greater in the commercial weldment that was evaluated (Ref 11), where a butter pass was used for this purpose. To determine the role of the grain-size microstructure of the base metal on the grain refinement or coarsening at the CGHAZ, two grain microstructures were selected. Microhardness values of 263 and 345 DPH were measured for the starting coarse-grain and fine-grain structures, respectively. The corresponding microstructures and carbide distributions are shown in Fig. 3 and 4.

3.1 *Metallurgical Changes in Gleeble Simulated HAZs*

The effect of each thermal cycle was assessed by examining grain-size variations and carbide distribution changes. Figure 5 summarizes the grain changes as a function of peak temperature for the two cycles employed. Figures 6 and 7 depict the microstructural variations associated with the grain changes recorded in Fig. 5. It was observed that the coarse-grain samples refined their grain microstructure as they were exposed to 950 and 1150 °C for a single cycle; the grains became coarser, however, when the peak temperature reached 1350 °C. The fine-grain base metal, on the other hand, experienced grain coarsening in every peak temperature at a single cycle, with the greatest coarsening at 1350 °C. In both base materials the double-cycle exposure to a lower temperature produced grain refinement of the structure with respect to the single cycle. Furthermore, with the exception of the double-cycle treatment at 950 °C, the original fine-grain microstructure was observed to have coarsened for every heat treatment. The coarse-grain structure, on the other hand, experienced grain refinement in every thermal cycle experience except for the 1350 °C single-cycle exposure.

In the case of the coarse-grain test specimens, only those samples exposed to 1350 °C and single cycled had a grain size larger than the original material. In the test samples exposed to the peak temperature of 950 °C, no significant changes were detected in the carbide population of the single cycle, and only slight coarsening of carbides occurred in the double cycle.

Concurrent with the carbide characterization, microhardness measurements of the microstructures were performed and are tabulated along with grain size in Table 3. The microhardness increase observed can be attributed somewhat to the grain refinement, but also to the increased carbon solid solution of the matrix due to some limited carbide dissolution. Exposure to the peak temperature of 1150 °C resulted in a bainitic micro-

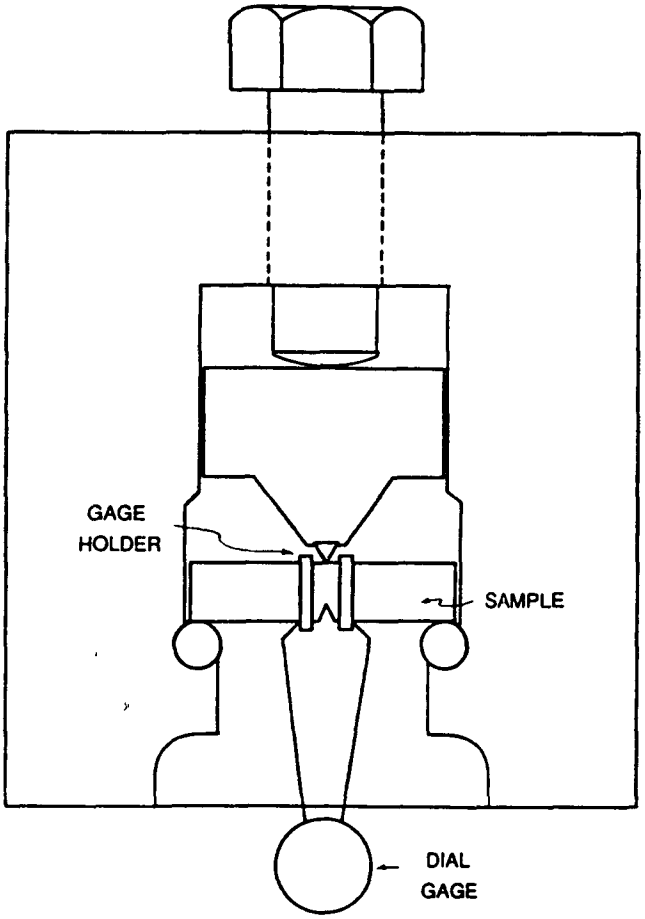

(a)

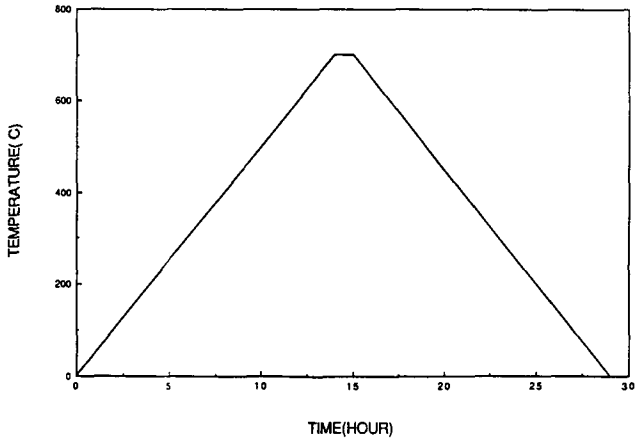

(b)

Fig. 2 (a) Three-point-bend notch-opening stress-relaxation test fixture. (b) Heat treatment applied to test samples loaded into the fixture in (a).

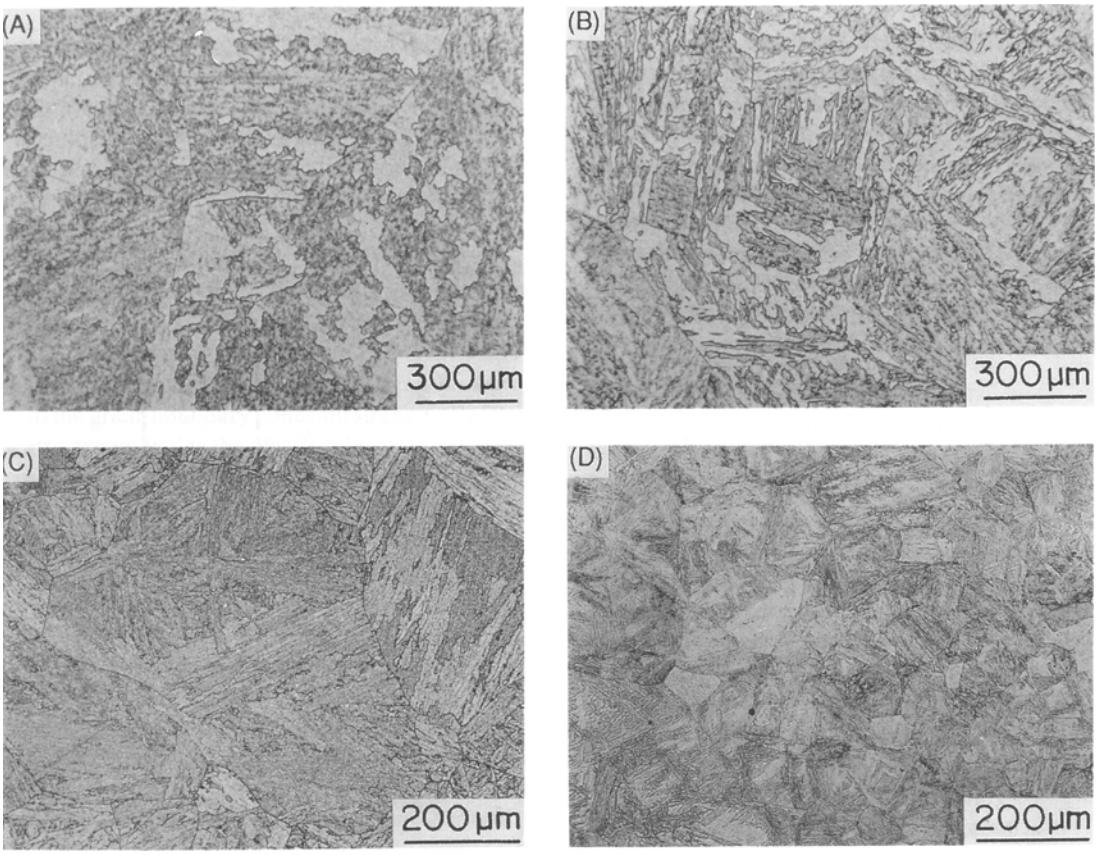

Fig. 3 Microstructures of base metals prior to Gleeble thermal cycles. (a) and (c) Coarse-grain structure. (b) and (d) Fine-grain structure

Table 3 Results of hardness and prior-austenite grain size measurements of the simulated HAZs

Base metal	Sample denomination	Peak temperature (°C)/cycle	Hardness, DPH	Grain size, μm
Coarse grain (ASTM No. 2.5, 155 μm, 263 DPH)	CG-950C-SC	950/single	314	28
	CG-950C-DC	950/double	276	<10
	CG-1150C-SC	1150/single	445	64
	CG-1150C-DC	1150/double	359	30
	CG-1350C-SC	1350/single	462	330
	CG-1350C-DC	1350/double	484	85
Fine grain (ASTM No. 5.5, 55 μm, 345 DPH)	FG-950C-SC	950/single	361	125
	FG-950C-DC	950/double	358	<10
	FG-1150C-SC	1150/single	368	90
	FG-1150C-DC	1150/double	372	75
	FG-1350C-SC	1350 /single	409	260
	FG-1350C-DC	1350/double	393	94

structure, with most of the original carbides dissolved and new fine carbides reprecipitated in the single cycle, corresponding to a microhardness increase to 445 DPH. The double cycle resulted in coarsening of these carbides and a drop in microhardness to 359 DPH.

Figures 8(a) and (b) depict the changes in carbide population just described. These samples were also observed by TEM; Fig. 9(a) shows the carbide population of the single-cycle specimen. Some of the original carbides are partially dissolved and appear spheroidized, but fine acicular carbides also are visible. The carbides for the 1150 °C/double-cycle treatment are coarser and more spheroidized (Fig. 9b). The coarse-grain test specimens single cycled at 1350 °C were bainitic with some martensite. The entire carbide population appeared to have gone into solution, and carbides could hardly be resolved by SEM (Fig. 10a). Even TEM could resolve only a few tiny carbides (Fig. 11a). In the case of the double cycle, the carbides become more obvious with SEM (Fig. 10b), indicat-

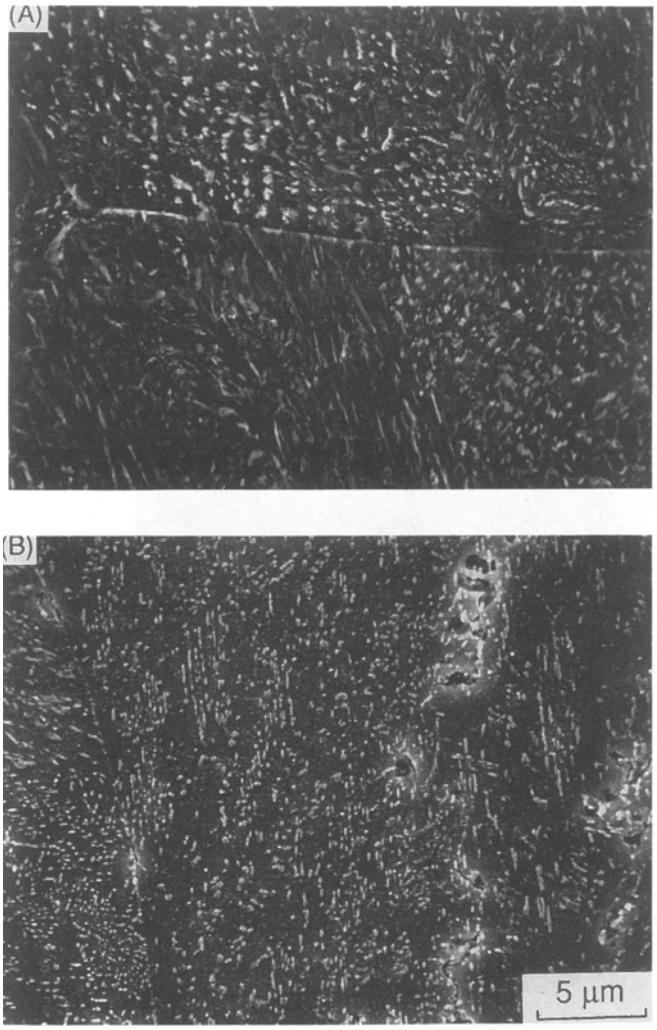

Fig. 4 SEM micrographs of base metals for HAZ simulation. (a) Coarse grain. (b) Fine grain

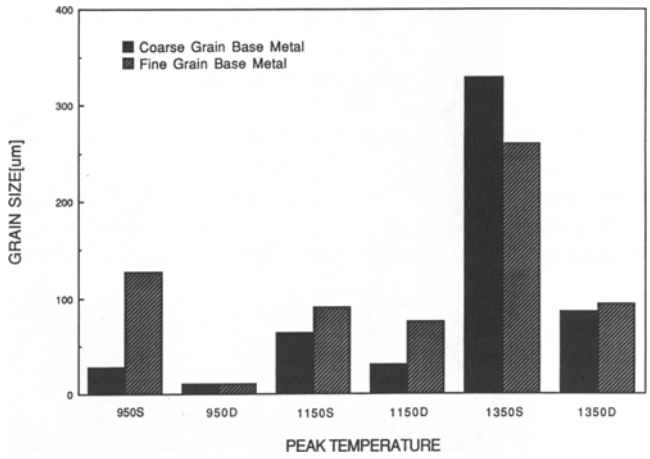

Fig. 5 Grain-size variation measured in simulated HAZs as a function of peak temperature and cycle number for the two base metals

ing greater reprecipitation of the carbides. The TEM micrograph for this particular specimen (Fig. 11b) shows few coarser carbides. The highest microhardness values were obtained for the last two samples cycled at 1350 °C; the slightly higher values observed for the double-cycle specimen are most likely due to its finer grain size (Table 3) and some carbide reprecipitation.

The fine-grain test specimens thermal cycled at 950 °C showed no significant changes in carbide structure. The test samples thermal cycled at 1150 °C, however, showed some coarsening and precipitation of interlath carbides, particularly in the sample that was double cycled. Figure 4 shows the original carbide distribution of the fine-grain base material, and Fig. 8(c) and (d) show the carbide structure after the Gleeble thermal cycles. The slight increase in microhardness to about 360 DPH experienced by the samples exposed to 950 °C (Table 3) could be attributed to some additional precipitation of very fine carbides not easily detected by SEM, but was most likely due to a limited carbide dissolution that led to an additional solid-solution strengthening of the matrix. It was also observed that the sample that was double cycled at 950 °C experienced grain refinement with no change in microhardness. This implies that carbide precipitation and the increase in carbon solid solution of the matrix are the controlling strengthening mechanisms. Additional carbide precipitation was better resolved in the 1150 °C samples, as noted earlier. The increase in microhardness was even higher, to around 370 DPH. The carbide changes and the increases in grain size and hardness became more obvious at the peak temperature of 1350 °C in the fine-grain material. It appears that most carbides dissolved and reprecipitated during these cycles, as shown in Fig. 10. The microhardness was measured at about 400 DPH.

The different microstructural changes in the simulated HAZs may be explained in terms of the competing effects of grain-growth kinetics and carbide dissolution on the bainite transformation and ultimately on the hardness of the final transformation product. Their net effect can be understood by analyzing the phenomenological changes caused by a thermal cycle. When the original bainitic microstructure transforms to austenite during heating, its grain growth is influenced by its kinetics, as well as by the grain-boundary pinning from the undissolved carbides in the matrix. Below a certain temperature, carbide dissolution is so limited that grain-boundary pinning becomes dominant and inhibits prior-austenite grain growth. This in turn depresses the start temperature of the bainite transformation. When the temperature increases above a critical value, carbide dissolution becomes more extensive, which in turn reduces or eliminates grain- boundary pinning. This, combined with the faster grain- growth kinetics at the highest temperature, results in very large grains. Such results were encountered in the microstructures exposed to the peak temperature of 1350 °C (single cycle). On the other hand, carbide pinning of the grain boundaries would be significant at the lower peak temperatures (950 and 1150 °C) because of the limited carbide dissolution and slower grain-growth kinetics.

In all cases, the double Gleeble cycle produced grain refinement due to the lower temperature kinetics, some intercritical phase transformations, and added grain boundary pinning from additional carbide coarsening.

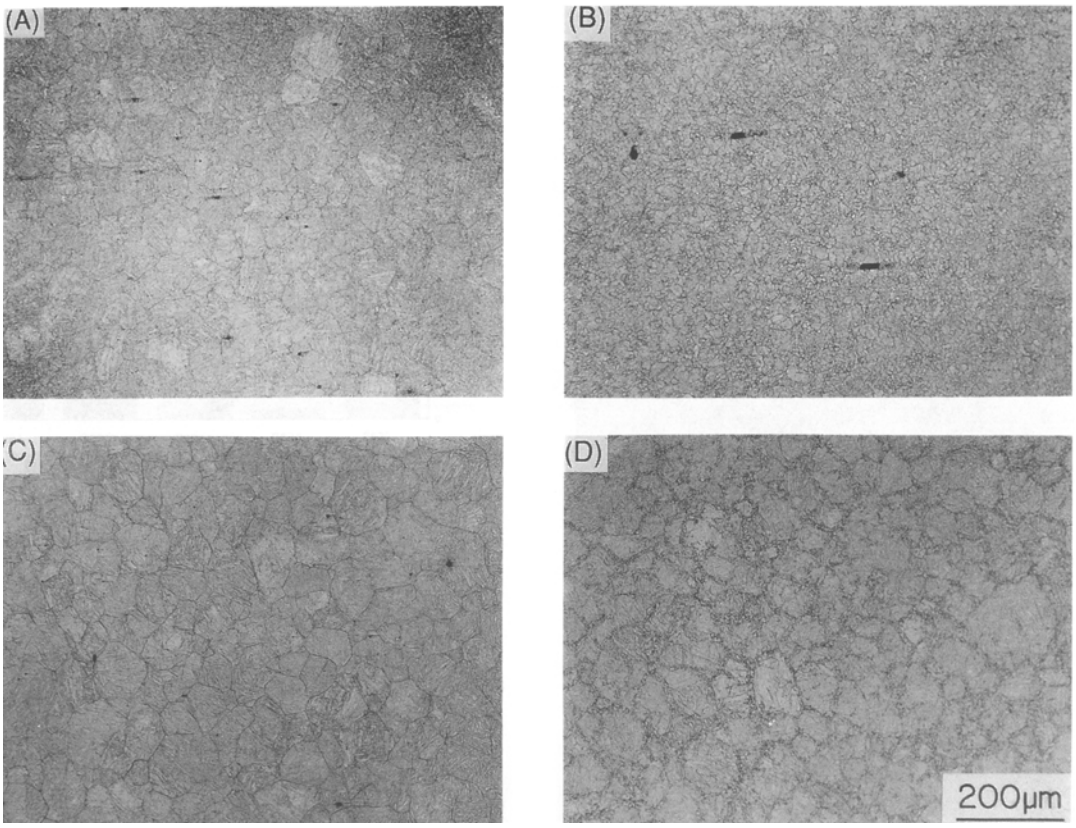

Fig. 6 Microstructure of simulated HAZ at 1150 °C peak temperature. (a) Coarse grain, single cycle. (b) Coarse grain, double cycle. (c) Fine grain, single cycle. (d) Fine grain, double cycle

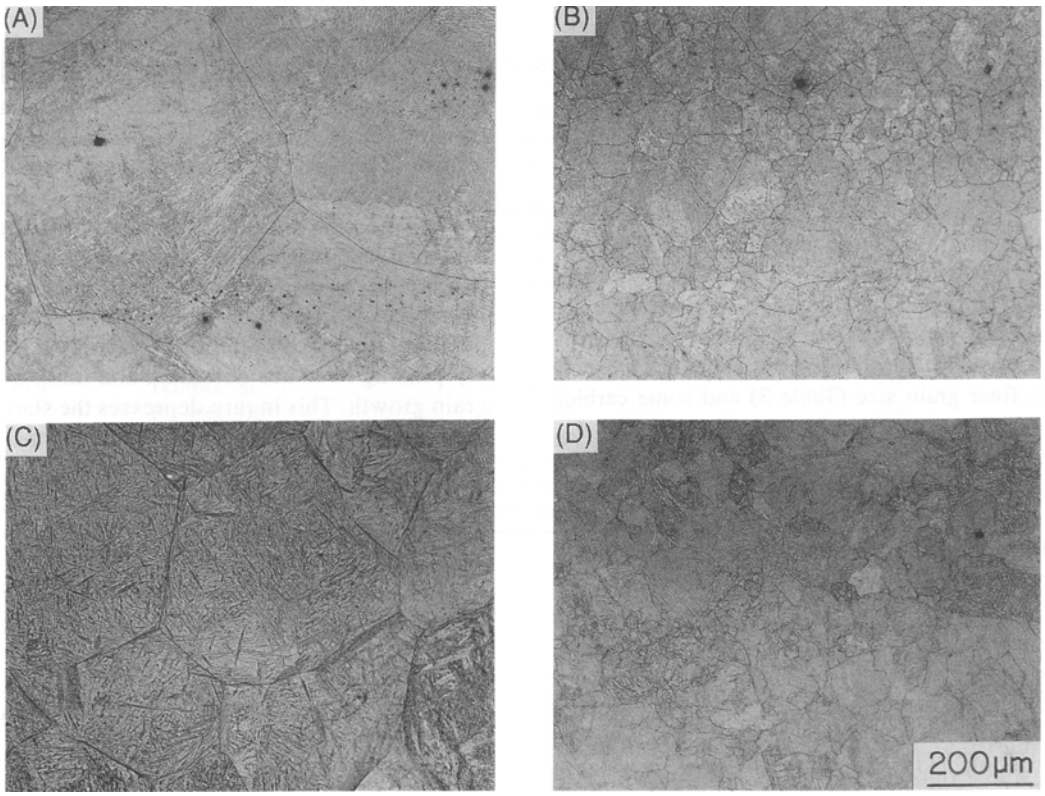

Fig. 7 Microstructure of simulated HAZ at 1350 °C peak temperature. (a) Coarse grain, single cycle. (b) Coarse grain, double cycle. (c) Fine grain, single cycle. (d) Fine grain, double cycle

3.2 *Reheat Cracking Test (Three-Point Bend Notch Opening Test)*

Residual and structural stresses also contribute to the development of reheat cracking, in addition to the metallurgical factors of grain size, microstructure, and carbide precipitation. Reheat cracking usually develops upon stress relieving of large pieces. In order to simulate the stresses (both residual and structural) experienced by the microstructure of a large piece, each sample was placed in the test fixture shown in Fig. 2(a) and stressed in bending to NODs of 50, 100, 200, and 300 μm. After inspecting the loaded samples to establish the absence of cracks, the entire fixture was loaded into the furnace and submitted to the stress-relief cycle shown in Fig. 2(b). After this procedure, the samples were unloaded and examined visually for possible cracks. All samples were also carefully examined under a microscope for any small cracking. Following these observations, all samples were submerged in liquid nitrogen

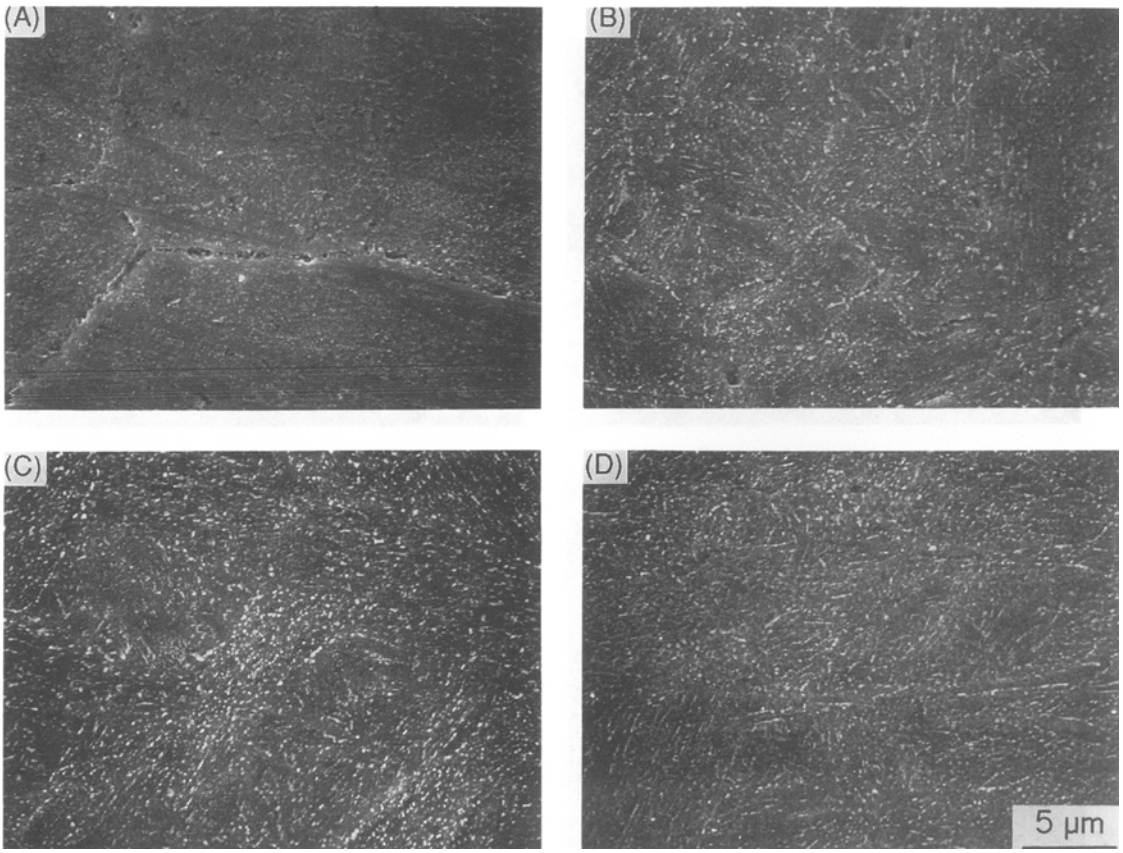

Fig. 8 SEM micrographs of simulated HAZ at 1150 °C peak temperature showing carbide distribution. (a) Coarse grain, single cycle. (b) Coarse grain, double cycle. (c) Fine grain, single cycle. (d) Fine grain, double cycle

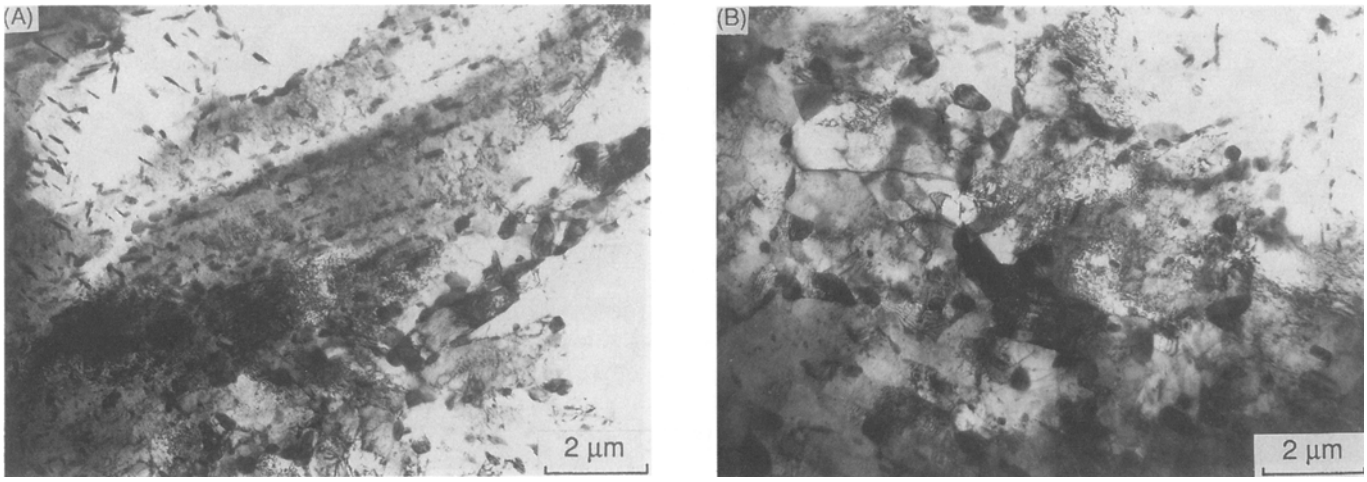

Fig. 9 TEM micrographs of simulated HAZ at 1150 °C. (a) Single cycle. (b) Double cycle

and immediately placed in a Charpy test machine for fracturing. The fracture surfaces of the samples were then analyzed by SEM for evidence of reheat cracking.

The results of the reheat cracking tests are summarized in Table 4. No cracking was observed in the simulated HAZs exposed to 950 °C, for both cycles and both base metals. Reheat cracking was detected in the two base metals when they were single cycled to 1150 °C (CG-1150C-SC and FG-1150C-SC). In case of the CG-1150C-SC test sample, cracking occurred despite refinement of the grain from 155 to 64 μm. The FG-1150C-SC specimens showed evidence of cavitation at the smallest strain, but then cracking became obvious in the 100 μm opening displacement. The grain structure in these test samples (FG-1150C-SC) was found to have coarsened from 55 to 90 μm. Note that sample CG-1150C-SC, despite having a finer grain (64 μm) than sample FG-1150C-SC (90 μm), appeared to be more susceptible to reheat cracking. The only difference between these samples was the microhardness values

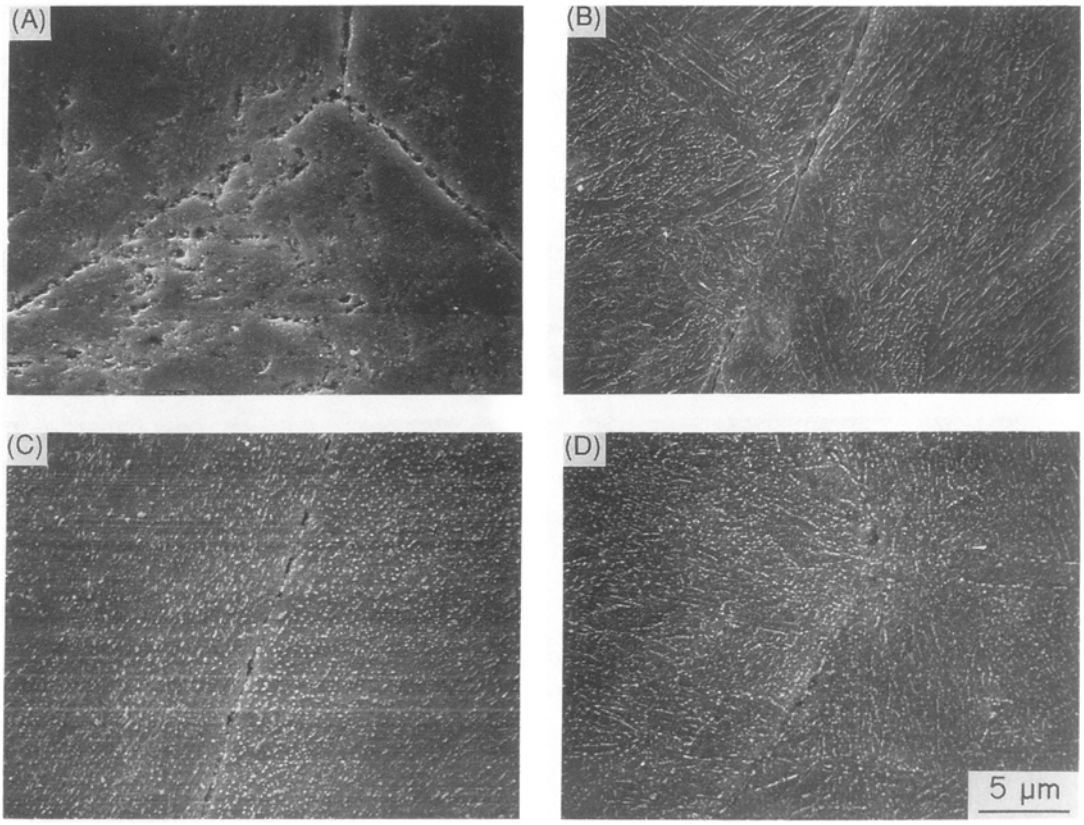

Fig. 10 SEM micrographs of simulated HAZ at 1350 °C peak temperature showing carbide distribution. (a) Coarse grain, single cycle. (b) Coarse grain, double cycle. (c) Fine grain, single cycle. (d) Fine grain, double cycle

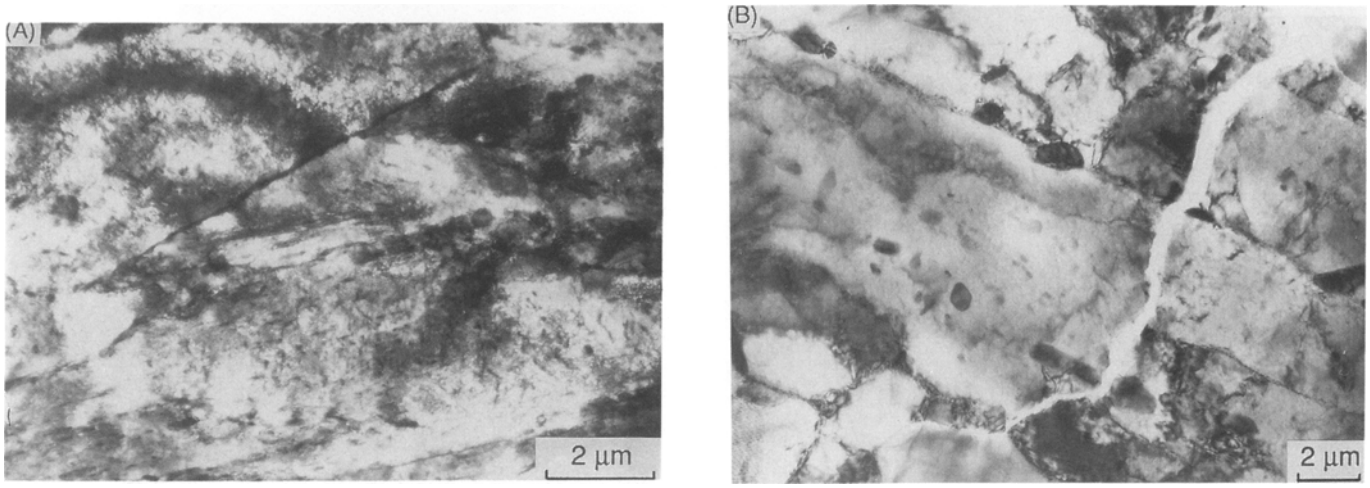

Fig. 11 TEM micrographs of the simulated HAZ at 1350 °C. (a) Single cycle. (b) Double cycle

(445 versus 368 DPH), probably caused by variation in carbide precipitation. It appears that a microhardness of approximately 370 DPH is critical even at small strains.

Samples CG-1350C-SC and CG-1350C-DC were very susceptible to reheat cracking; CG-1350-SC had a much coarser grain (330 μm), compared to the original base metal (155 μm), and its

Table 4 Results of reheat cracking tests in the simulated HAZs

Peak temperature (°C)/cycle	Sample denomination	NOD, μm 50	100	200	300
Coarse-grain base metal					
950/single	CG-950C-SC	(a)	(a)	Safe	Safe
950/double	CG-950C-DC	(a)	(a)	Safe	Safe
1150/single	CG-1150C-SC	Crack	Crack	(a)	(a)
1150/double	CG-1150C-DC	(a)	Safe	Safe	(a)
1350/single	CG-1350C-SC	Crack	(a)	Crack	(a)
1350/double	CG-1350C-DC	Crack	Crack	(a)	(a)
Fine-grain base metal					
950/single	FG-950C-SC	(a)	Safe	Safe	(a)
950/double	FG-950C-DC	(a)	Safe	Safe	(a)
1150/single	FG-1150C-SC	Safe?(b)	Crack	(a)	(a)
1150/double	FG-1150C-DC	(a)	Safe	Safe	(a)
1350/single	FG-1350C-SC	Crack	Crack	(a)	(a)
1350/double	FG-1350C-DC	(a)	Safe?(b)	Safe?(b)	(a)

(a) No testing. (b) Initiation of void formation

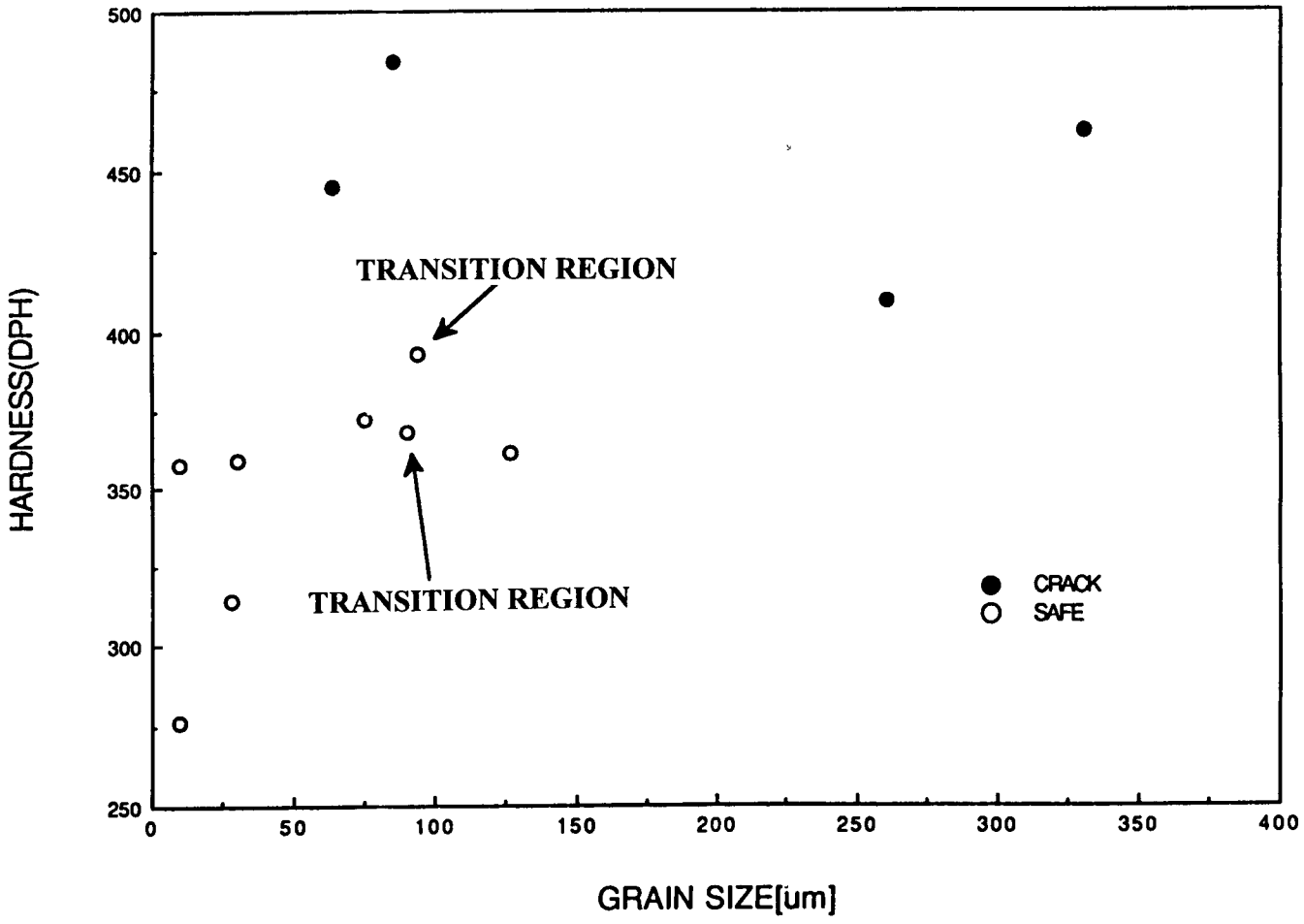

Fig. 12 Mapping defining approximate ranges of reheat cracking in terms of grain size and hardness of the simulated HAZs

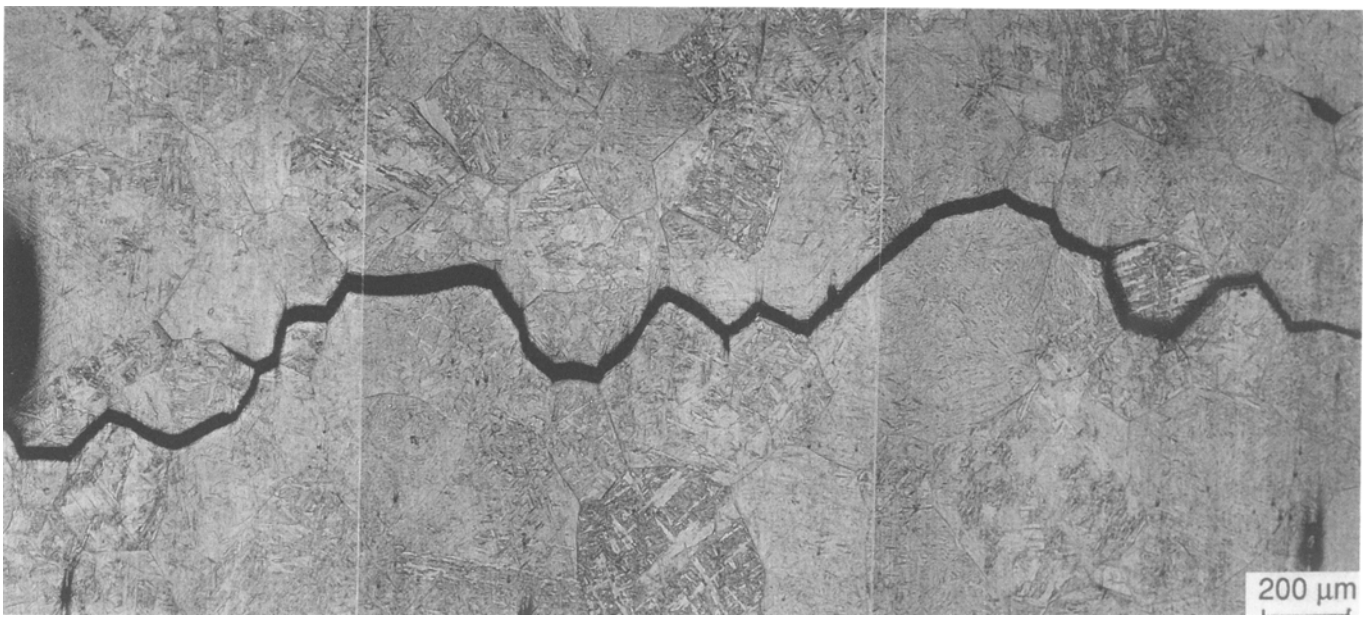

Fig. 13 Typical reheat crack on simulated HAZ from 1350 °C peak temperature. Single cycle for the coarse-grain base metal

microhardness value increased by 200 points to 462 DPH. Apparently, the solid-solution strengthening of the matrix by the carbides going into solution, plus the precipitation strengthening due to the reprecipitation of new fine carbides, combined to increase microhardness. Similar structure changes had occurred in sample CG-1350C-DC, yet greater carbide reprecipitation and some coarsening were observed. In addition, this sample experienced grain refinement, which could have possibly contributed to a further increase in hardness.

The results of Tables 3 and 4 were plotted in Fig. 12 in terms of grain size and hardness to define an approximate range of reheat cracking. This map shows that a combination of coarse grain and high hardness would result in reheat cracks. Control of grain size alone does not guarantee elimination of these cracks. Based on the results shown in Fig. 12, the HAZs of CrMoV steels with microhardness values of less than 370 DPH and prior-austenite grain sizes of less than about 80 μm would not experience reheat cracking.

Reheat cracking is known to occur intergranularly, as shown in Fig. 13. The crack initiated at the notch tip. All the test samples that cracked during the three-point bend test exhibited intergranular fracture. A typical feature of reheat cracks in early stages is void formation, as shown in Fig. 14. It was indicated earlier that grain refinement alone could not control reheat cracking; Fig. 15 shows SEM micrographs for two samples with similar high hardness, but one having a grain-size structure five times smaller than the other. Note that both micrographs show the typical intergranular crack mode. Sample CG-1150C-SC shows a secondary crack branching from the primary crack (Fig. 15b).

3.3 *Interpretation of Reheat Cracking Behavior of Samples*

Based on the microstructural changes of the carbide distribution in connection with the peak temperatures of the thermal cycles, it is apparent that only thermal cycling at the two highest peak temperatures had a significant effect on carbide dissolution and reprecipitation. For instance, for the coarse-grain base material, the 1150 and 1350 °C heat treatments produced the largest increases in microhardness (Table 3). Much of the hardness increase of the grain matrix can be attributed to carbide (precipitation) strengthening and most probably is caused by the development of coherent carbide precipitates. Such microhardness increases would stiffen the grain interior. When these test specimens are subjected to notch bending tests, the stress relaxation they experience due to the servicelike conditions induces deformations that are primarily confined to the grain boundaries. If the strain induced as a result of this relaxation exceeds the available grain-boundary ductility, then intergranular failure will occur. This grain-boundary deformation is manifested in the extensive cavity formation at the subgrain boundaries of the 1350 °C HAZ shown in Fig. 14. Following cavitation or void formation, cracking will develop due to the eventual coalescence of these cavities.

Microhardness measurements were also performed on some samples after the reheat crack test. Microhardness drops of 88 and 142 DPH, respectively, were observed in samples CG-1350C-SC and CG-1350C-DC, and both specimens experienced reheat cracking. Specimen CG-1150C-SC had a hardness drop of 85 DPH and also experienced reheat cracking; however, no reheat cracking was observed in sample CG-1150-DC, and a hardness drop of only 33 DPH was measured. The coarse-grain samples submitted to the peak temperature of 950 °C experienced microhardness drops of 35 and 25 DPH for the single and double cycles, respectively. Neither of these two last samples showed reheat cracking. These results imply that samples experiencing hardness matrix drops greater than 80 DPH underwent reheat cracking. Phenomenological or mechanistic explanations for developing a model for reheat cracking have not yet been established. However, important mechanical and metallurgical correlations have been defined.

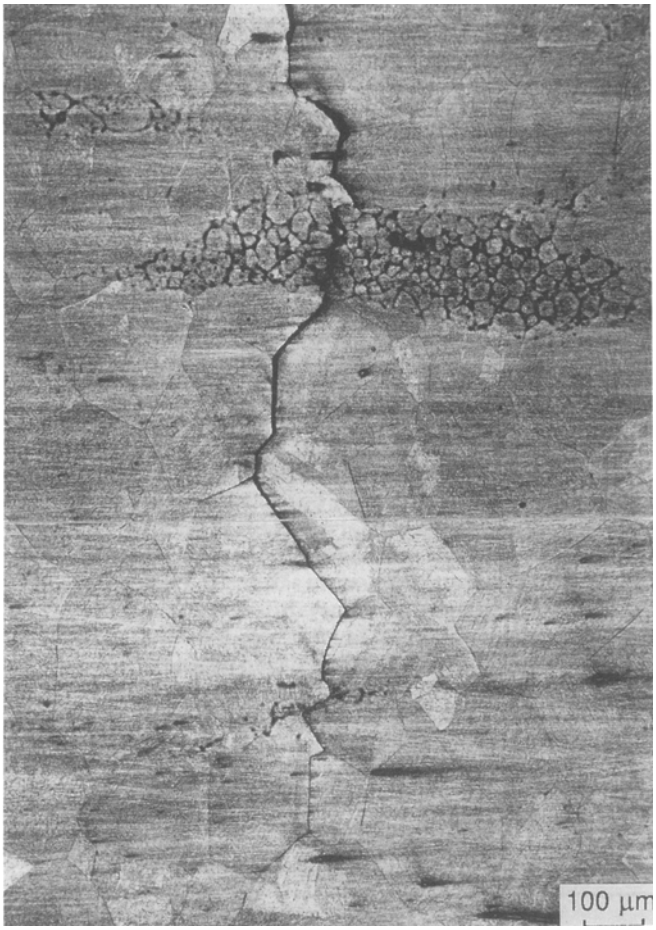

Fig. 14 Reheat crack with extensive cavity formation at subgrain boundaries on simulated HAZ from 1350 °C peak temperature. Single cycle for the coarse-grain base metal

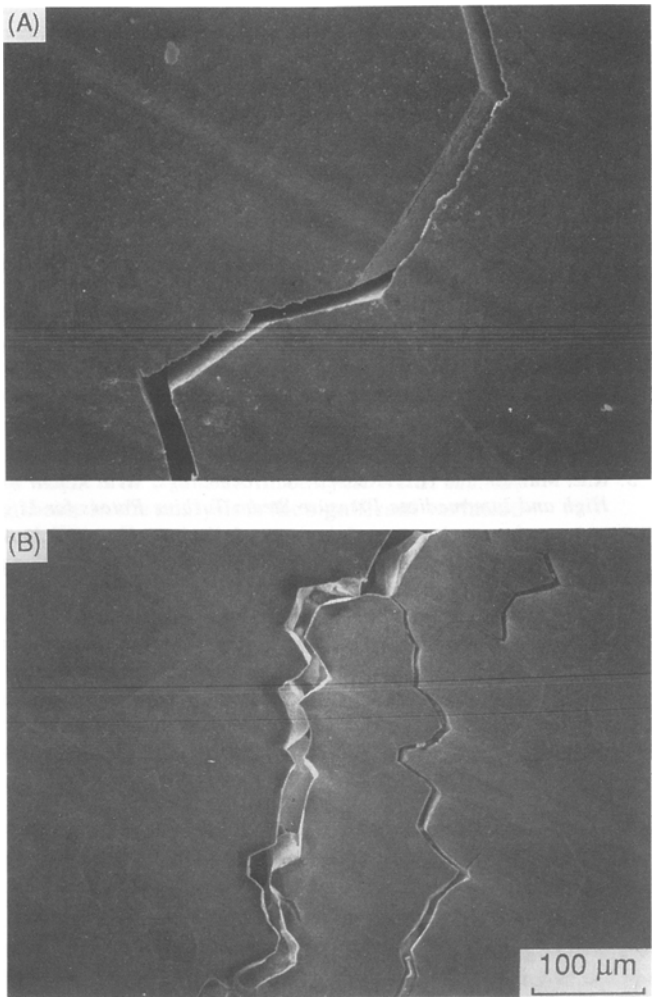

Fig. 15 SEM micrographs of reheat cracks on simulated HAZs for the coarse-grain base metal. (a) Single cycle at 1350 °C. (b) Single cycle at 1150 °C

4. Conclusions

Two grain-size microstructures of the same steel were used as the starting base material in an evaluation of the metallurgical and mechanical factors that cause reheat cracking in CrMoV rotor steels. Testing was conducted using Gleeble simulated HAZs. Of the three peak temperatures selected for thermal cycling, 1350 °C was the temperature expected at the CGHAZ; peak temperatures of 1150 and 950 °C were selected to determine whether reheat cracking was limited to the CGHAZ. The effect of a second cycle also was assessed, since turbine weld repair involves multipass welding. The following conclusions were reached:

- Reheat cracking susceptibility was most significant at the highest peak temperature. No reheat cracks were found in the test samples exposed to the peak temperature of 950 °C.
- Reheat cracking was found to depend not only on prior-austenite grain size but also on the microhardness of the grain matrix of the simulated HAZ. It was found that reheat cracking of the CGHAZ is controlled if the microhardness is below 350 DPH and the prior-austenite grain size is less than 80 µm.
- The test specimens exposed to a single thermal cycle at 1350 °C underwent extensive carbide dissolution, unrestricted grain growth, and fine carbide reprecipitation on cooling. The samples exposed to 950 °C underwent partial reaustenitization and very limited carbide dissolution, which inhibited grain growth. The 1150 °C single-cycled specimens also experienced reheat cracking, accompanied by significant carbide dissolution and controlled grain growth.
- As expected, the second cycle at lower temperature reduced the susceptibility to reheat cracking in all cases because of grain refinement and some reduction of matrix microhardness and carbide coarsening. The original grain size of the base materials appears to play no role in the reheat crack susceptibility of the HAZ.
- Ultimately, reheat cracking in the HAZ of CrMoV rotor steels can be eliminated by properly controlling the weld fabrication process to ensure a grain-refined structure and optimum matrix microhardness.

References

1. S.H. Bush, Failures in Large Steam Turbine Rotors, *Proceedings: Rotor Forgings for Turbines and Generators,* EPRI WS-79-235, Electric Power Research Institute, 1981, p 1-1 to 1-27
2. R.T. Hagaman, Failures Experience with Generator Rotors, *Proceedings: Rotor Forgings for Turbines and Generators,* EPRI WS-79-235, Electric Power Research Institute, 1981, p 1-32 to 1-39
3. J. Byron, in *Proceedings: Weld Repair of High and Intermediate Pressure Steam Turbine Rotors for Life Extension,* EPRI GS-6233, Electric Power Research Institute, 1989, p 5-6
4. S. Bayard, P.A. Coulon, and M. Nougaret, in *Proceedings: Weld Repair of High and Intermediate Pressure Steam Turbine Rotors for Life Extension,* EPRI GS-6233, Electric Power Research Institute, 1989, p 2-15 to 2-27
5. R.E. Munson and N.D. Russell, in *Proceedings: Weld Repair of High and Intermediate Pressure Steam Turbine Rotors for Life Extension,* EPRI GS-6233, Electric Power Research Institute, 1989, p 1-40 to 1-54
6. R.E. Clark, J.M. Schmerling, D.R. Amos, and L.D. Kramer, Experience with Weld Repair of Low Pressure Steam Turbine Rotors, *Proceedings: American Power Conference,* Illinois Institute of Technology, Chicago, IL, 1985.
7. V.N. Zemzin and R.Z. Shron, *Avtom. Svarka,* Vol 21 (No. 6), 1968, p 1
8. N.T. Burguess, *Weld. Met. Fabr.,* Vol 30, 1962, p 105
9. K.P. Bently, *Br. Weld. J.,* Vol 11, 1964, p 507
10. G.S. Kim, J.E. Indacochea, and T.D. Spry, Metallurgical Aspects in Welding CrMoV Turbine Rotor Steels—Part 1: Evaluation of Base Material and Heat Affected Zone, *J. Mater. Sci. Technol.,* Vol 7, 1991, p 42-49
11. G.S. Kim, J.E. Indacochea, and T.D. Spry, Metallurgical Aspects in Welding CrMoV Turbine Rotor Steels—Part 2: Evaluation of Narrow-Gap Submerged-Arc Weldment, *J. Mater. Sci. Technol.,* Vol 7, 1991, p 147-154